Kinetics of Intercalation of Lithium and Sodium into $(PbS)_{1.14}(NbS_2)_2$

L. Hernán, J. Morales,* L. Sánchez, and J. L. Tirado

Laboratorio de Química Inorgánica Facultad de Ciencias, Universidad de Córdoba, San Alberto Magno s/n, E-14004 Córdoba, Spain

Received November 30, 1992. Revised Manuscript Received June 7, 1993

The electrochemical and transport properties of the intercalation of Li and Na into $(PbS)_{1.14}(NbS_2)_2$, a misfit layer compound, have been investigated. The open-circuit voltage (OCV) of the lithium cell gradually decreases with increasing lithium content, while the OCV of $Na_x(PbS)_{1.14}(NbS_2)_2$ shows the appearance of a voltage plateau in the range of composition $0.1 < x < 0.25$. This different behavior has been correlated with the chemical diffusion coefficients obtained by a long-pulse galvanostatic technique. While the chemical diffusivity of lithium increased with composition and had a maximum of $\sim 1.3 \times 10^{-9}$ cm^2 s^{-1} for composition $0.4 < x < 0.5$, the diffusion coefficients of Na^+ were found to decrease slowly in the range $0.05 < x < 0.2$, where the voltage–composition curve showed a two-phase region supported by the related X-ray data. On the other hand, the standard free energies of intercalation for sodium intercalates are less negative than those found for the respective lithium intercalated compounds.

Introduction

In recent years, studies on the chemical and physical properties of intercalation compounds have proliferated on account of both their technological significance in various fields including battery and sensor development, and the academic interest of their unusual structural properties. Thus, a number of transition metal dichalcogenides have been used as host materials to increase the available knowledge on the primary effects of intercalation: structural changes and charge transfer from the guest species to the host.[1,2] However, these two effects are mutually related since structural changes on insertion are affected by electron transfer processes.

In this context, the synthesis of new layered materials suitable for intercalation reactions may provide further information on the nature of intercalation phenomena. Such is the case with the more complex chalcogenide systems such as misfit layer chalcogenides, the earliest of which were synthesized some 20 years ago.[3] Their structures were recently elucidated from single-crystal X-ray diffraction measurements. An excellent review of the structural and transport properties of these compounds was recently published by Wiegers and Meerschaut.[4] Of special interest to intercalation studies is the family of nonstoichiometric composition $(MS)_{1+x}(TS_2)_2$ (M = Sn, Pb, Bi; T = Ti, Nb, Ta). So far, the crystal structure has only been determined for $(PbS)_{1.18}(TiS_2)_2$[5] and $(PbS)_{1.14}(NbS_2)_2$.[6] The structure of the latter compound can be described in terms of two orthorhombic PbS and NbS_2 sublattices stacked along the c axis and incommensurate along the a axis. One salient feature of this structure is that each |PbS| slab is separated by two consecutive $|NbS_2|$ sandwiches, thus providing a typical van der Waals gap between these consecutive NbS_2 slabs, which can be occupied by electron releasing species.

Lithium and sodium were recently shown to be intercalated chemically or electrochemically into these systems.[7-11] However, to acquire a coherent understanding of the mechanisms involved in these intercalation processes, a fundamental knowledge of the driving forces and kinetic parameters that come into play is required. This paper has a 2-fold aim, namely, (a) to evaluate the chemical diffusivity of alkali ions in intercalates of nominal composition $A_x(PbS)_{1.14}(NbS_2)_2$ (A = Li, Na), kinetic parameters (viz. the chemical diffusion coefficient $\tilde{D}(x)$) and the thermodynamic or Darken factor $K_t(x)$ being obtained from long-pulse galvanostatic titration curves, and (b) to calculate the standard free energy of the intercalation reaction. The results are correlated with the structural features of the materials.

Experimental Section

The studied compound was prepared by heating the constituent elements Pb, Nb, and S in a 1:2:5 proportion in evacuated quartz ampules under identical conditions that were described elsewhere.[6] According to X-ray diffraction, electron microscopic and X-ray energy dispersive analysis data, the material was obtained as high-purity platelike particles with a metal luster.

A two-electrode cell consisting of an alkali metal disk anode and a compacted $(PbS)_{1.14}(NbS_2)_2$ cathode of ~20 mg of active material were used for electrochemical experiments. The electrolyte used was a 1 M solution of $MClO_4$ (M = Li, Na) (Merck) dissolved in propylene carbonate that was previously distilled in vacuo. Cells were assembled and discharged under an argon atmosphere in an M-Braun glovebox. The water content inside

(1) Whittingham, M. S. *Prog. Solid State Chem.* **1978**, *12*, 41.
(2) Whittingham, M. S.; Jacobson, A. J., Eds.; *Intercalation Chemistry*; Academic Press: New York, 1982.
(3) Sterzel, W. Z. *Naturwiss.* **1966**, *53*, 199.
(4) Wiegers, G. A.; Meerschaut, A. *Sandwiched Incommensurate Layered Compounds*; Meerschaut, A., Ed.; Trans Technical Publishers: Zurich, 1992.
(5) Meerschaut, A.; Auriel, C.; Rouxel, J. *J. Alloys Compounds*, **1992**, *183*, 129.
(6) Meerschaut, A.; Guemas, L.; Auriel, C.; Rouxel, J. *Eur. J. Solid State Inorg. Chem.* **1990**, *27*, 557.
(7) Auriel, C.; Meerschaut, A.; Deniard, P.; Rouxel, J. *C. R. Acad. Sci. Paris.* **1991**, *313 Ser. II*, 1255.
(8) Hernán, L.; Lavela, P.; Morales, J.; Pattanayak, J.; Tirado, J. L. *Mater. Res. Bull.* **1991**, *26*, 1211.
(9) Lavela, P.; Morales, J.; Tirado, J. L. *Chem. Mater.* **1992**, *4*, 2.
(10) Barriga, C.; Lavela, P.; Morales, J.; Pattanayak, J.; Tirado, J. L. *Chem. Mater.* **1992**, *4*, 1021.
(11) Hernán, L.; Morales, J.; Pattanayak, P.; Tirado, J. L. *J. Solid State Chem.* **1992**, *100*, 262.

0897-4756/93/2805-1167$04.00/0

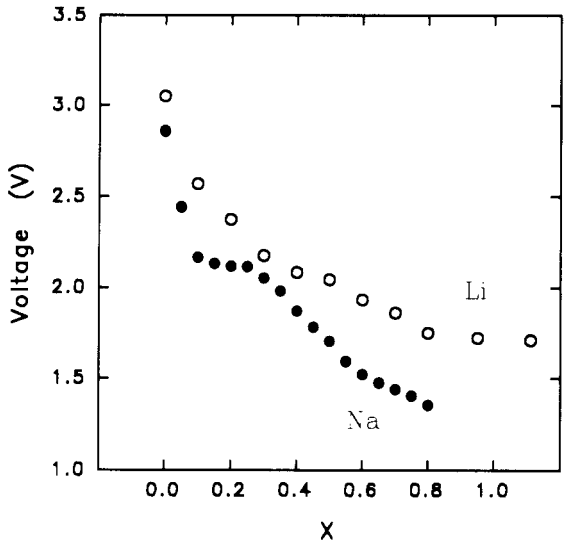

Figure 1. Open-circuit voltage values vs composition x for lithium and sodium insertion in $A_x(PbS)_{1.14}(NbS_2)_2$ (A = Li, Na).

the box was monitored with a humidity sensor and turned out to be 2–3 ppm H_2O. Cells were discharged galvanostatically on an Amel-549 potentiostat/galvanostat. Open-circuit voltage (OCV) composition curves were obtained by coulometric titration. Constant current densities between 6 and 20 $\mu A/cm^2$ for sodium and 15–100 $\mu A/cm^2$ for lithium were applied to the cells for preset times so as to transfer known amounts of lithium and sodium into the crystals. The average alkali metal composition of the cathodic material was calculated from Faraday's law on the assumption that no current flow was due to side reactions. After each titration, the cells were allowed to stand at open circuit to allow equilibrium to be restored, which was assumed to occur when the cell voltage changed by less than 1 mV in 2 h. For the determination of diffusion coefficients, 0.105–0.125-mm-thick $(PbS)_{1.14}(NbS_2)_2$ pellets were prepared and current pulses in the range 6–15 $\mu A/cm^2$, which resulted in discharges of 0.05 F were used. Discharge periods between 8–22 h were applied in order to fulfill the condition $\tau > 0.25$ ($\tau = \tilde{D}t/\delta^2$, where $\tilde{D}$ is the chemical diffusion coefficient and δ the thickness). Relaxation periods were interrupted when voltage changes dropped below 1 mV/h.

Results and Discussion

Open-circuit voltage composition curves are shown in Figure 1 and were obtained in duplicate experiments performed at room temperature. The voltage of Li/$(PbS)_{1.14}(NbS_2)_2$ cell is a smooth decreasing function of the intercalation degree, x, in the composition range $0 < x < 1$ and is similar to that reported by Auriel et al.[7] A subtle change in the slope occurs between $x = 0.4$–0.5. This anomaly in the voltage discharge curve was previously found to occur in other systems (particularly in electrochemical measurements on the Li/TiS_2 cell),[12] and its structural origin is still a subject of debate. Different authors[12–14] have correlated this electrochemical feature with the formation of superstructures as a results of Li^+ ions arranging themselves in octahedral sites of the TiS_2 host. However, this interpretation contrasts with the ^{77}Se NMR results reported for Li_xTiSe_2 by Chabre and Deniard[15] that indicate only short-range ordering of Li^+ ions. For lithium compositions close to one, our results

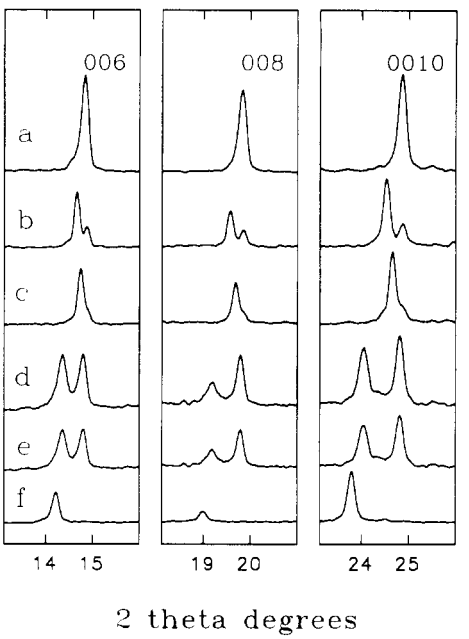

Figure 2. Selected 00l profiles in the X-ray powder diffraction patterns of (a) pristine $(PbS)_{1.14}(NbS_2)_2$, (b) and (c) $Li_{0.2}(PbS)_{1.14}(NbS_2)_2$ before and after equilibrium, (d) and (e) $Na_{0.2}(PbS)_{1.14}(NbS_2)_2$ before and after equilibrium, and (f) $Na_{0.5}(PbS)_{1.14}(NbS_2)_2$.

are markedly divergent of those reported by Auriel et al.[7] These authors found that the voltage fell rapidly with increasing x. In our case, no such sharp voltage drop occurred, but the voltage remained virtually constant at 1.7 V. A similar behavior was also observed for the Li/$(PbS)_{1.18}(TiS_2)_2$ cell,[10] whose OCV discharge curve showed an extended plateau of 2.0 V in the composition region $1.0 \leq x \leq 2.0$. The coexistence of noncrystalline decomposition products and intercalated misfit layer compounds may account for an extended plateau once the octahedral sites (one per formula unit) are fully occupied.

The intercalation of Na leads to lower voltage values than those provided by the lithium cell. Moreover, the profile of the voltage–composition curve is markedly different from that of lithium cell. We should emphasize the occurrence of a clear plateau in the composition range $0.1 < x < 0.25$, where the voltage and hence the chemical potential of sodium remain virtually constant. At higher sodium contents, the voltage changes almost linearly up to a degree of intercalation close to 0.6. A subtle break in the slope occurs at a degree of intercalation of 0.65. Sodium contents greater than 0.9 result in the decomposition of the starting misfit layer structure into poorly crystallized phases.[16]

The X-ray diffraction pattern of partly intercalated samples provided additional information on the structural changes undergone by the host lattice during the intercalation process (Figure 2). The powder XRD pattern of $(PbS)_{1.14}(NbS_2)_2$ shows several strong peaks which are multiple-order reflections of the basal planes and few weak peaks. Because the X-ray diffraction lines other than (00 l) are rather weak probably owing to preferred orientations—for the alkali metal intercalates these lines practically disappear—we only calculate the c-axis parameter. The observed d spacings for each (00 l) reflection of pristine

(12) Thompson, A. H. *Phys. Rev. Lett.* **1978**, *40*, 1511.
(13) Berlinsky, A. J.; Unruh, W. G.; McKinnon, W. R.; Haering, R. R. *Solid State Commun.* **1979**, *31*, 135.
(14) Hibma, T. *J. Solid State Chem.* **1980**, *34*, 97.
(15) Chabre, Y.; Deniard, P. *Chemical Physics of Intercalation*; Legrand, A. P., Flandrois, S., Eds.; *NATO ASI Series* **1988**, *B172*, 387.
(16) Hernán, L.; Morales, J.; Sánchez, L.; Tirado, J. L. *Solid State Ionics* **1992**, *58*, 179.

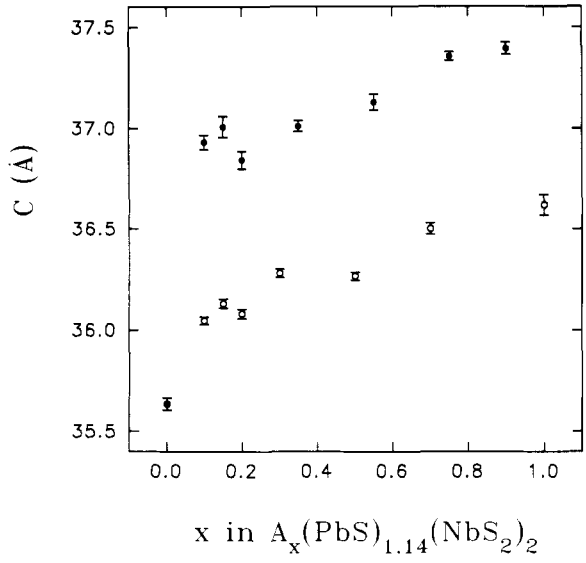

Figure 3. Plot of the *c*-axis dimenson as a function of alkali-ion content in $A_x(PbS)_{1.14}(NbS_2)_2$. A = Li (○), Na (●).

sample were used to calculate the average *c* unit cell parameter to be 3.564$_7$ nm. This value is consistent with a unit cell including two PbS and four NbS_2 slabs forming an NbS_2–NbS_2–PbS–NbS_2–NbS_2–PbS repeating unit along the [001] direction.[6]

A significant finding is the concurrence of pristine and sodiated phases at a discharge depth $x = 0.2$ for a cathodic material that was allowed to stand 1 month in order to reach equilibrium. For this intercalate, Figure 2e, the XRD pattern shows double lines in the positions where multiple-order reflections of the basal spacing would be expected. The first set of lines is consistent with the presence of the pristine phase, while the second set leads to the *c* parameter of a sodium intercalated phase plotted in Figure 3. In contrast, although a freshly prepared cathodic material with a lithium content of 0.2 also showed concurrent unlithiated and lithiated phases (Figure 2b), on standing for a few hours, the double peak yielded by the sample became a single peak lying at intermediate 2θ value (Figure 2c). This may account for the differences between the discharges curves of the two cells and the two-phase mechanism for the electrochemical sodiation of $(PbS)_{1.14}(NbS_2)_2$ in the range $0.11 < x < 0.2$ arising from slow diffusion of Na^+ ions across the network.

On the other hand, an increase in the *c*-axis with increase in the discharge depth was observed (Figure 3), which can be an indication that the alkali ions are located at the interface between NbS_2/NbS_2 and/or PbS/NbS_2 lamellae. The *c* values reported here for $Li_x(PbS)_{1.14}(NbS_2)_2$ are in good agreement with the values obtained by Auriel et al.[7] The results of sodium intercalates show a dependence on *x* similar to that of lithium compound and a difference of ca. 0.8 Å is calculated from the *c* values of both intercalates. This value is in agreement with the difference in size of both ions.

Unfortunately, the axis dimensions in the *ab* plane could not be obtained from such data as a result of a strong preferred orientation of the particles that gave rise to enhanced intensities of the [00 *l*] reflections and the virtually complete disappearance of other reflections including *h* and/or *k* components. However, the electron diffraction data for [001] zones suggest little changes in the *ab* plane (Figure 4). These electron diffraction patterns are characterized by two set of spots corresponding to the two sublattices associated with PbS and NbS_2 layers. Also, the reciprocal cells had a^* axes of unequal length, consistent with the incommensurate character of both sublattices. The electron diffraction patterns of the intercalated phases are very similar to that of the pristine phase and do not show the phenomena frequently observed in samples lithiated chemically for short periods, consistent with the development of an apparent 12-fold symmetry. This behavior has been interpreted in term of changes in the orientation of the slabs arising from the distortions induced by the incoming ions.[8]

According to the classification proposed by Armand for intercalation electrodes,[17] $Li_x(PbS)_{1.14}(NbS_2)_2$ system behaves like a nonstoichiometric type I compound. The electrode potential can be evaluated taking into account ionic and electronic contributions and adding a term for the interaction between guest ions. In contrast, "$Na_x(PbS)_{1.14}(NbS_2)_2$" system approaches the category of pseudo-two-phase type II compounds. The larger size of Na^+ requires a greater expansion of the *c* dimension and consequently the strains induced in the host lattice by the intercalation process increase. This situation can be expressed as a strong positive interaction term that would lead to a maximum in the voltage–composition curve. This unstable system has a tendency to stabilize through a disproportionation reaction with the appearance of a plateau in the voltage–composition curve due to the equilibrium of the two pseudophases.

Diffusion coefficients were calculated by using the method of Honders et al.,[18] which is a modified version of the galvanostatic intermittent titration technique (GITT) developed by Weppner and Huggings.[19] It features two major advantages that are worth emphasizing. It allows both chemical diffusion coefficients and the thermodynamic factors to be calculated by using transient measurements, without the need for the slope of the O.C.V. curve (steady-state measurements), and avoids potential difficulties occasionally involved in evaluating this parameter. In addition, the method requires no prior knowledge of the electrode surface area, which is difficult to determine in pressed powdered samples (partly owing to electrolyte penetration phenomena).[20] In fact, diffusivity is reportedly a function of the effective surface area.[21] The cathode surface is substituted by its thickness, which should give rise to no appreciable errors in assessing kinetic properties of mixed solid conducting electrodes.[22] In the last few years, the Honders method has been successfully applied to the determination of the diffusion coefficient of Li^+ in various positive electrodes.[22-24] Thus, for the Li/TiS_2 cell, one system that can be used as a test cell, the values provided by this method are consistent with those

(17) Armand, M. B. *Materials for Avanced Batteries*, Murphy, D. W., Broadhead, J., Steele, B. C. H., Eds.; *NATO Series* **1980**, 145.
(18) Honders, A.; Der Kinderen, J. M.; Van Heeren, A. H.; Wit, J. H. W.; Broers, G. H. J. *Solid State Ionics* **1985**, *15*, 265.
(19) Weppner, W.; Huggins, R. A. *J. Electrochem. Soc.* **1977**, *124*, 1569.
(20) Spurdens, P. C.; Steele, B. C. H. *Solid State Ionics* **1986**, *21*, 151.
(21) Yamamoto, T.; Kikkawa, S.; Koizumi, M. *Solid State Ionics* **1985**, *17*, 63.
(22) Pistoia, G.; di Vona, M. L.; Tagliatesta, P. *Solid Solid Ionics* **1987**, *24*, 103.
(23) Chang, S. H.; Menetrier, M.; Delmas, C.; Chaminade, J. P. *J. Electrochem. Soc.* **1991**, *138*, 1209.
(24) Julien, C. *Microionics Solid State Integrable Batteries*; Elsevier Science Publishers: Amsterdam, 1991; p 309.

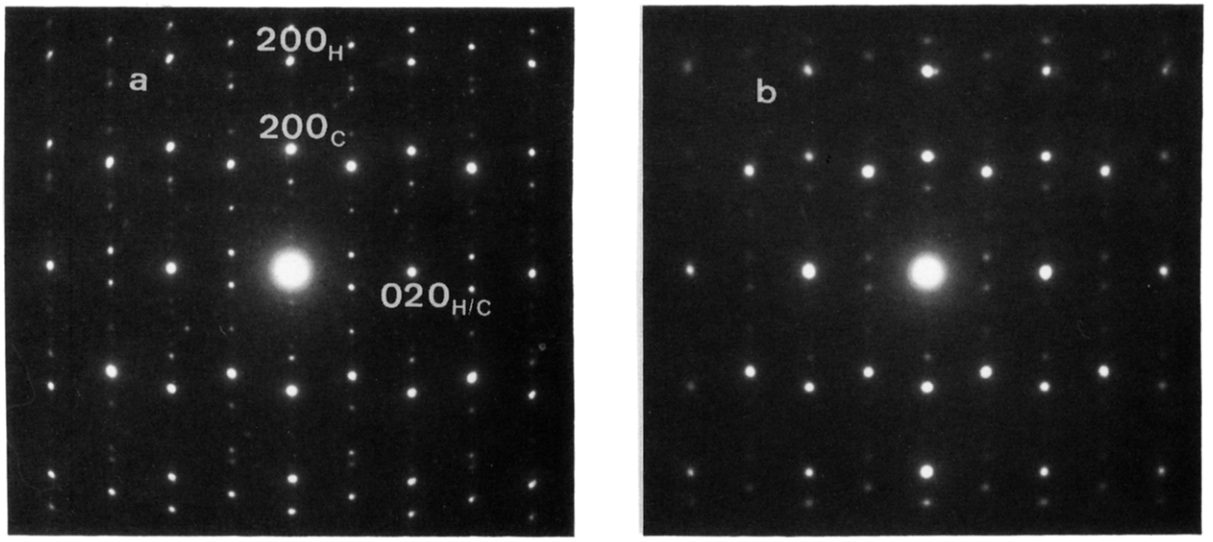

Figure 4. Experimental [001] zone electron diffraction pattern of pristine $(PbS)_{1.14}(NbS_2)_2$ before (a) and after (b) sodium intercalation.

obtained by the method developed by Basu and Worrell[25] or the galvanostatic intermittent titration technique.[26]

The method is based on the analysis of the relaxation periods which follow a long time galvanostatic current pulse through a Li/electrolyte/intercalation electrode cell. When the conditions $\tau_{pulse} > 0.25$ and $\tau_{decay} < 0.25$ are fulfilled (where $\tau = \tilde{D}t/\delta^2$) the time dependence of the cell voltage can be expressed as

$$\Delta E(t) = -(IK_tRT/AF^2C^*)[2(t/\pi\tilde{D})^{1/2} - (t/\delta)] \quad (1)$$

where K_t is the thermodynamic factor, c^* is the alkali-metal concentration, I the current pulse, A is the surface area, δ is the cathode thickness, and R, T, and F have their usual meaning.

For small relaxation time values, t/δ is negligible, and according to eq 1 ΔE follows a square-root of time law. For larger values of time, the contribution of the second term in equation is significant. Honders et al.[18] assume that the difference $\Delta E'$ between ΔE and the straight line obtained by extrapolating the linear part of the ΔE vs $\sqrt{t}$ plot varies linearly with time according to the expression

$$\Delta E' = IRTK_tt/AF^2C^*\delta \quad (2)$$

Thus, the thermodynamic factor K_t can be evaluated from the slope of the $\Delta E'$ vs t plot, and the chemical diffusion coefficient $\tilde{D}$ from the slope of ΔE vs $\sqrt{t}$ and $\Delta E'$ vs t by the expression

$$\tilde{D} = 4/\pi[\delta(d\Delta E'/dt)/(d\Delta E/\sqrt{t})]^2 \quad (3)$$

Figure 5 shows some typical $\Delta E/\sqrt{t}$ and $\Delta E'/t$ plots.

Figure 6 shows the chemical diffusion coefficients of $A_x(PbS)_{1.14}(NbS_2)_2$ (A = Li, Na) in terms of alkali-metal contents. The results of the diffusion coefficients determination were carried out by successive galvanostatic titrations on the same cell for different x values. This was repeated three times with different cells and the three sets of measurements were used to compute the average value of $\tilde{D}$ and its standard deviation for each x. For lithium intercalation the diffusivity is low for concentrations close to 0 and 1 and peaks at $\sim 1.3 \times 10^{-9}$ cm^2 s^{-1} for

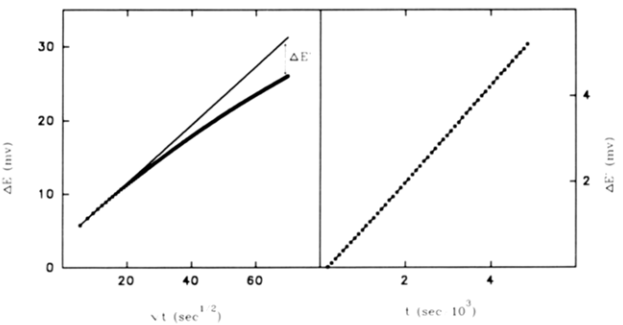

Figure 5. Typical ΔE vs $\sqrt{t}$ and $\Delta E'$ vs t plots for $Li_x(PbS)_{1.14}(NbS_2)_2$, $x = 0.25$, temperature = 25 °C, pulse time = 8 h 42 min, $I = 5.5$ μA ($\Delta x = 0.05$), $\delta = 0.0112$ cm, $\tau = 0.33$. (■) Experimental data, (—) tangent line in ΔE vs $\sqrt{t}$ plot, (- - -) regression line in $\Delta E'$ vs t.

compositions in the range $0.4 < x < 0.5$ are observed. However, at compositions greater than $x = 0.8$, the data deviate from this trend, probably as a result of a significant loss of long-range ordering in the misfit structure, as revealed by a sharp decrease in the intensities of the X-ray diffraction peaks. Unfortunately, a literature scan failed to provide any data regarding diffusion coefficient values for lithium in NbS_2. In fact, most available data are referred to Li/TiS_2 system[18,21,24-26] and, to lesser extent to the Li/TaS_2 system.[25] As a rule, the reported values for these binary systems are greater than those found in this work by 1 or 2 orders of magnitude.

The thermodynamic factor K_t evaluated from kinetic data (the slope of the $\Delta E'/t$ curve, eq 2) can be compared with that obtained by stationary measurements. In this case, K_t can be derived from the relation[18]

$$K_t = -(xF/RT)(dE/dx) \quad (4)$$

By determination of the slope of the coulometric titration curve (dE/dx) at different stoichiometries, the thermodynamic factor may be obtained as a function of the degree of intercalation (x). The K_t values obtained from kinetic and stationary measurement data are shown in Figure 7. As can be seen, the two sets of values are quite consistent, which can be taken as indirect proof of the reliability of the method and the significance of the diffusion coefficient sequence.

Also, this quantity was found to increase in the domain $0.05 \leq x \leq 0.8$ and reach a value of 33.3 at $x = 0.75$. These

(25) Basu, S.; Worrell, W. L. *Fast Ion Transport in Solids*; Vashista, P., Mundy, J. N., Shenoy, G. K., Eds.; Elsevier: Amsterdam, 1979; p 149.
(26) Kanehori, K.; Kirino, F.; Kudo, T.; Miyauchi, K. *J. Electrochem. Soc.* **1991**, *138*, 2216.

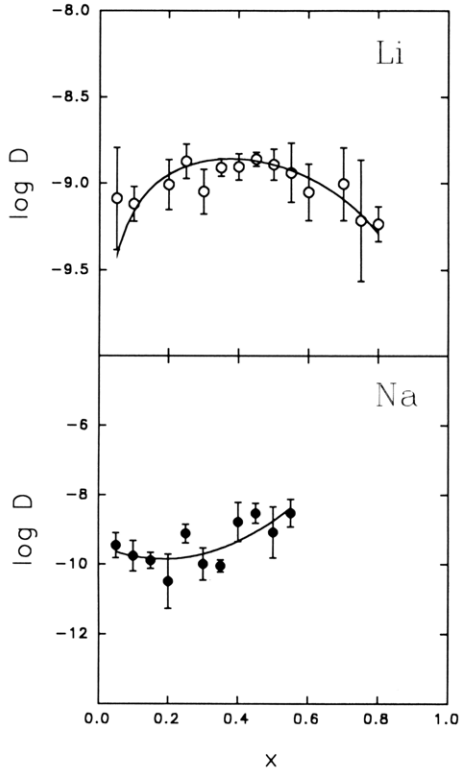

Figure 6. Compositional variation of the chemical diffusion coefficient ($cm^2\ s^{-1}$) of Li^+ and Na^+ intercalated into $(PbS)_{1.14}(NbS_2)_2$.

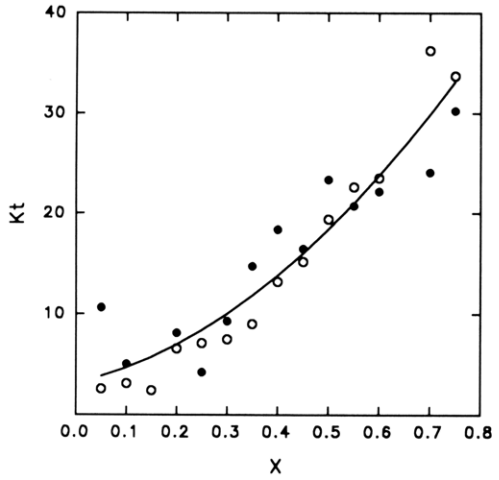

Figure 7. Compositional variation of the thermodynamic enhancement factor for $Li_x(PbS)_{1.14}(NbS_2)_2$, as determined from kinetic (○) and stationary (●) measurements.

are approximately twice the reported values for $Li_xTi_{1.03}S_2$.[24] Such large K_t values have been ascribed to strong electrostatic repulsion between inserted ions.[27]

Although there is no direct evidence for the location of the alkali metal in the host matrix, simple geometrical considerations suggest that the guest ions would first occupy the octahedral positions in the van der Waals gap between adjacent NbS_2 slabs. A projection of the structure of the misfit along the *b* axis is shown in Figure 8. Full occupancy of these octahedral vacant sites would lead to a nominal composition $Li(PbS)_{1.14}(NbS_2)_2$. Higher lithium contents would involve the occupancy of the tetrahedral sites in the van der Waals gap formed at the NbS_2/NbS_2 interface not shown in Figure 8 and/or the distorted tetrahedral sites at the NbS_2/PbS interface. However, recently reported results[11] have shown the difficulty of obtaining alkali-metal intercalates of misfit layer compounds of nominal stoichiometry MTX_3 owing to interlayer interactions and the small size and irregular geometry of the sites that affect consecutive MT–TX_2 slabs. Thus, according to this diffusion model the alkali metal would move from one octahedral site to the adjacent site, passing by a neighboring tetrahedral site lying at the same distance from both octahedral sites. On the basis of the likelihood of a jump between these vacant positions taking place, Nagelberg[28] derived an equation that relates chemical diffusivity and the composition *x*:

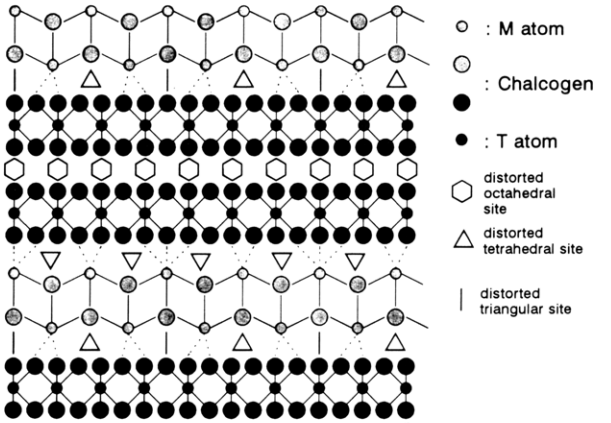

Figure 8. Idealized projection along [010] of a layered chalcogenide with a misfit of MX and TX_2 (X: chalcogen) sublattices along [100].

$$\tilde{D} \propto [e^P x^2(1-x) + x(1-x)^2] \qquad (5)$$

where e^P is a constant which depends on the energy of interaction between neighboring intercalated alkali atoms ($P = -\Delta E_a/RT$). According to eq 5, at small interaction energy values ($\simeq$0 kcal), e^P is close to unity and the diffusion coefficient peak is at $x = 0.5$, whereas at large ($\geq$5 kcal), $e^P \simeq 0$ and the $\tilde{D}$ maximum is at $x = 0.33$. As the experimental data collected in Figure 6 fluctuate somewhat, a definitive conclusion of the position of the $\tilde{D}$ maximum cannot be directly obtained. However, an estimate of the repulsive interaction energy was computed by curve fitting eq 5 to the experimental data. The resulting function is plotted in Figure 6 as a solid line for a value of $e^P = 0.232$ that can be converted in a value of interaction energy of about 0.9 kcal. This value is reasonably consistent with that reported for the Li_xTaS_2 system[29] and with that recently published by Julien[24] for the $Li_xTi_{1.005}S_2$ system.

If the chemical diffusion coefficient is determined by the mobility of one type of ionic species, then the partial ionic conductivity of alkali ions (σ_A) can be calculated from the above-mentioned parameters by using an equation developed by Weppner and Huggins:[19]

$$\sigma_A = nF\tilde{D}/(dx/dE)V_m \qquad (6)$$

with *n* being the amount of electrons involved in the charge

(27) Armand, M. B. *Fast Ionics Transp. Solids* **1973**, 665.

(28) Nagelberg, A. S. Ph.D. Thesis, University of Pennsylvania, Philadelphia, 1978; p 127.

(29) Nagelberg, A. S.; Worrell, W. L. *Proc. Symp. Electrode Materials and Processes for Energy Conversion and Storage*; McIntyre, J. D. E., Srinivasau, S., Will, F. G., Eds.; Electrochemical Society: Princenton, NJ, 1977; p 847.

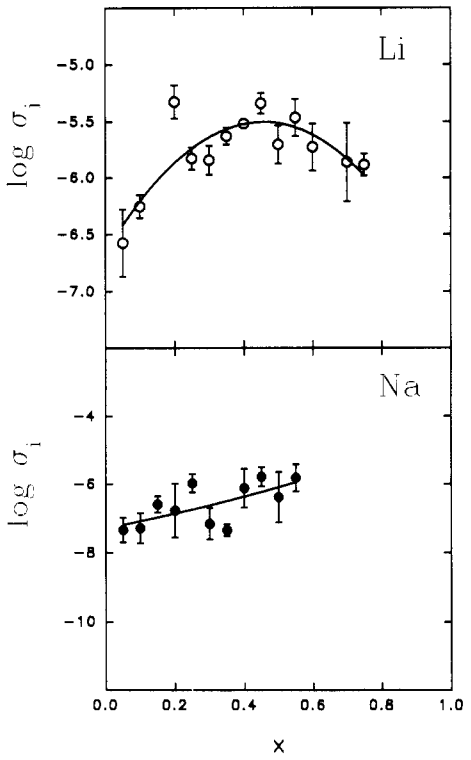

Figure 9. Changes in lithium and sodium ionic conductivities (Ω^{-1} cm^{-1}) with composition in $(PbS)_{1.14}(NbS_2)_2$.

transfer process, F is the Faraday constant, V_m is the molar volume of composition x of the phase considered, and dE/dx is the slope of the voltage vs composition plot at x.

Estimating the molar volume of misfit layer compounds is somewhat more complex than in simpler phases owing to the presence of two sublattices with unit cell parameters that are incommensurate in one crystallographic direction. According to recent single crystal determinations, the unit cell parameters of each orthorhombic sublattice in the compound $(PbS)_{1.14}(NbS_2)_2$ here studied are as follows:[6]

PbS part (C): $a = 5.829$ Å, $b = 5.775$ Å, $c = 35.861$ Å, $Z = 8$

NbS_2 part (H): $a' = 3.326$ Å, $b' = 5.776$ Å, $c' = 35.876$ Å, $Z = 8$

On the assumption that changes in the unit cell parameters through alkali-metal intercalation affect c and c' only, the molar volume per exact formula unit in pristine and intercalated products is thus $a'b'c'N/4$, where N is Avogadro's number. Figure 9 shows the variation of the partial conductivity as a function of the degree of intercalation in $Li_x(PbS)_{1.14}(NbS_2)_2$. The parabolic shape of the compositional variation plot is similar to that for TiS_2[24] and provides a maximum average value of 4.5×10^{-6} Ω^{-1} cm^{-1} at compositions close to $x = 0.45$.

Figure 6 shows the variation of the chemical diffusion coefficient, $\tilde{D}$, as a function of the sodium ion concentration. As can be seen, the plot differs somewhat from that for lithium intercalation. Since sodium intercalation takes place by a two-phase mechanism in the first stages of reaction, the values of $\tilde{D}$ are not comparable with those of Li in that composition range. The diffusion coefficient was found to decrease gradually over the composition range $0.05 \le x \le 0.2$. As the guest concentration increased, the diffusion coefficient increased with sodiation up to a sodium content of $x = 0.6$. Further sodiation resulted in considerable distortion of the host lattice and widely variable diffusion coefficient values.

Most reported chemical diffusion coefficients for monovalent metals in transition metal chalcogenides show that the mobility increases slightly with increasing degree of intercalation. This has been related to the expansion of the interlayer distance caused by the intercalation process, on the assumption that such an expansion promotes diffusivity. This explanation is not universally applicable, as shown by the transport properties of lithium-intercalated $NiPS_3$ recently reported by Julien et al.[30] The chemical diffusion coefficient of this system increases with increasing lithium content up to $x = 0.4$ in spite of the fact that the interlayer distance remains constant upon intercalation of lithium.[31] In our case, a significant Δc-parameter expansion normal to the slabs of the host structure occurred (Figure 3).

Winn et al.[32] reported a reduction of sodium diffusivity in $Na_xTi_{1.002}S_2$ at $0.42 < x < 0.46$ which was ascribed to the presence of excess titanium in the van der Waals gap. However, this suggestion is inapplicable to Figure 6 since a similar effect on lithium diffusivity should be expected. This uncommon behavior can be better understood by taking into account the shape of the equilibrium potential composition curve (Figure 1). Emf values lie on a constant voltage plateau over the composition range $0.1 < x < 0.25$, which corresponds to a two-phase region. Although the Honder method for estimating diffusion coefficient does not explicitly require a single-electrode process, the kinetics of this system obviously involve a coupled phase transformation process, opening of the unoccupied gaps between NbS_2 sandwiches and diffusion. Thus the overvoltage observed must be due to a combination of both processes that introduce some uncertainly in the diffusion rate measurements.

However, the X-ray diffraction patterns of the cathodic material and the sequence of chemical diffusivity values are surprisingly consistent. Thus, for a composition close to $x = 0.2$, where the chemical diffusion coefficients are smaller, the cathodic material behaves as a two-phase system consisting of sodiated and unsodiated diffraction domains. At higher sodium contents, where the chemical diffusion coefficient is also higher, only a single phase is detected.

Figure 9 shows the variation of the ionic conductivity of sodium ions as obtained from eq 6 with the sodium ion concentration. Again, the compositional dependence of the partial conductivity is somewhat different from that exhibited by the lithium intercalates as a result of the complexity of the $Na/(PbS)_{1.14}(NbS_2)_2$ system. The ionic conductivity tends to increase with increasing x and reaches an average value of about 10^{-6} Ω^{-1} cm^{-1} at a composition of $x = 0.6$. This is comparable to the values obtained for the lithium ion conductivity in spite of the size difference. Indeed, the reported ionic conductivity of lithium and sodium in other host materials are quite similar (e.g. single-crystal V_6O_{13})[20,33] notwithstanding the fact that lithium diffusivity is somewhat higher.

(30) Julien, C.; El-Farth, L.; Balkanski, M.; Samaras, I.; Saikh, S. I. *Mater. Sci. Eng.* **1992**, *B14*, 127.
(31) Lemehaute, A.; Ouvrard, G.; Brec, R.; Rouxel, J. *Mater. Res. Bull.* **1977**, *12*, 1191.
(32) Winn, D. A.; Schemiet, J. M.; Steele, B. C. H. *Mater. Res. Bull.* **1976**, *11*, 559.
(33) Munshi, M. Z. A.; Smyrl, W. H.; Schmidtke, C. *Chem. Mater.* **1990**, *2*, 530.

The open circuit voltages shown as a function of x in Figure 1 were used to derive the Gibbs free energy function for the intercalation reaction:

$$xA(s) + (PbS)_{1.14}(NbS_2)_2(s) \rightarrow A_x(PbS)_{1.14}(NbS_2)_2(s) \quad (7)$$

The standard Gibbs free energy of this reaction can be evaluated as a function of composition by integration of the titration curve, according to the following expression:[34]

$$\Delta G^\circ_I = -F\int_0^x E\,dx \quad (8)$$

which is simply Faraday's constant times the area under the voltage–composition curve from the pure chalcogenide to the intercalated compound. The ΔG°_I values for lithium and sodium intercalation are listed in Table I. The lithium intercalates have more negative standard free energies of intercalation than do the sodium intercalated compounds, which is consistent with the general trend of the free energy of intercalation of alkali metals in transition dichalcogenides.[28] In addition, the results in Table I are roughly 10% smaller than those reported for these binary systems.

This result, together with the lower chemical diffusion coefficients compared with those of binary chalcogenides, support the idea that misfit layer sulfides can be regarded as intercalation compounds in which MS layers are inserted into the van der Waals gap of a layered transition metal disulfide. In fact some X-ray photoemission and X-ray absorption spectroscopy results[35] suggest the occurrence of a charge-transfer process from the MS layer to the transition-metal disulfide slabs. This electron release process would polarize the sulfur ions and raise an energy barrier that would hinder access of incoming alkali ions.

Table I. Free Energy of Intercalation for $A_x(PbS)_{1.14}(NbS_2)_2$ (A = Li, Na)

	ΔG (kJ mol^{-1})	
x	$Li_x(PbS)_{1.14}(NbS_2)_2$	$Na_x(PbS)_{1.14}(NbS_2)_2$
0.1	− 26.7	− 23.9
0.2	− 49.6	− 44.5
0.3	− 70.9	− 54.7
0.4	− 91.5	− 73.8
0.5	−111.5	− 91.0
0.6	−130.8	−106.5
0.7	−149.5	−121.0
0.8	−167.4	−134.5
0.9	−184.6	−147.4
1.0	−201.3	

Acknowledgment. We express our gratitude toward the CICYT (Contract MAT 88-007708) and Fundación Ramón Areces for the financial support of this work.

(34) Nagelberg, A. S.; Worrell, W. L. *J. Solid State Chem.* **1979**, *29*, 345.

(35) Ohno, Y. *Phys. Rev. B.* **1991**, *44*, 1281.